Engineering Transactions, **70**(3): 203–220, 2022, doi: 10.24423/EngTrans.2036.20220801
Institute of Fundamental Technological Research Polish Academy of Sciences (IPPT PAN)
Université de Lorraine • Poznan University of Technology

ICEM•2022

On the Strain Rate Sensitivity of Fibre-Reinforced Self-Compacting Concrete

Małgorzata PAJĄK[1)*], Jacek JANISZEWSKI[2)]

[1)] *Silesian University of Technology, Department of Structural Engineering*
Gliwice, Poland

[2)] *Military University of Technology*
Warsaw, Poland; e-mail: jacek.janiszewski@wat.edu.pl

[*]Corresponding Author e-mail: malgorzata.pajak@polsl.pl

This study investigates the characteristics of self-compacting concrete (SCC) reinforced with recycled fibres and their combination with polypropylene fibres, which can be applied to build protective structures. The split Hopkinson pressure bar (SHPB) method was used to subject the mixtures to high strain rates in the range from 140 to 200 s^{-1}, corresponding to impact loads. It was found that the strain rate sensitivity of both types of mixtures was comparable. The failure pattern confirmed the role of fibres in carrying the loads for strain rates below around 100 s^{-1}.

Key words: split Hopkinson pressure bar; recycled steel fibres; self-compacting concrete.

1. Introduction

Concrete reinforced with randomly distributed short fibres is considered to be the best material to withstand high stresses generated by explosions, impacts, or natural hazards. It has the potential to be used in protective structures (e.g., protective shelters, bunkers, barriers) or civil infrastructure (e.g., bridges, tunnels) [1]. The incorporation of fibres into the brittle cement-based matrix can effectively improve its post-cracking behaviour under quasi-static and dynamic loading conditions. This is associated with the mechanism of the transformation of the load from the matrix to the fibres and the bridging effect [2, 3].

It is well known that cement-based materials are strain-rate sensitive, which is manifested by a pronounced increase in their compressive strength and ability to absorb energy with an increase in strain rate [1–17]. The strain rate dependency of the growing micro-cracks and the viscosity of the bulk concrete between the cracks are mainly responsible for the enhancement of material parameters

over a low and moderate range of strain rates. Meanwhile, the structural effects are mainly regarded to be responsible for the increase of mechanical properties of the material over the ranges of strain rates higher than 10 s^{-1} [18]. However, the influence of various factors such as the compressive strength of the matrix on the strain rate sensitivity of cement-based materials, is often contradictory [4]. For this reason, more research is needed in this field.

Among the different types of fibres, the steel ones are considered to significantly improve the mechanical properties of the brittle matrix. The ecological equivalent of industrial steel fibres was considered in this paper. The fibres used in the investigation came from end-of-life tyres. Waste tyres represent a huge environmental problem as their number increases year by year, the amount of space needed for their storage is significant, and they are highly susceptible to fires [6]. In general, recycled fibres are characterised by a more curved shape and stochastic length and diameter in comparison to manufactured fibres [7, 8]. Any research proving their effectiveness in the concrete matrix can contribute to their practical application.

The split Hopkinson pressure bar (SHPB) technique is widely applied to investigate the high strain rate response of brittle materials [8–17, 19]. The effects influencing these results, such as friction, inertia, or elastic wave dispersion, have been analysed by many researchers to increase their validity [20–22]. Indeed, the influence of micro-straight and hooked steel fibres on the strain rate sensitivity of cement-based matrix has been widely analysed in recent publications [11–14]. Meanwhile, recycled fibres have only been investigated by Chen *et al.* [8] and by the authors of this paper [9, 10]. The volume ratio of applied steel fibres does not exceed 2% and it is associated with the workability of the matrix, which decreases with the addition of fibres. Most of the analyses indicated a decrease in the strain rate dependency of the matrix related to the incorporation of the fibres [9, 12, 13, 15, 17]. The SHPB tests were performed on different cement-based matrices for strain rates reaching 330 s^{-1}. In the tests where the strain rates did not exceed 130 s^{-1}, the addition of the fibres slightly improved the strain rate sensitivity of the matrix [8]. However, examples of laboratory test results are available in the literature in which fibre-reinforced self-compacting concrete (SCC) was more strain rate sensitive than plain SCC [11, 14]. Therefore, the role of the fibres in matrices subjected to high strain rate loads requires further studies.

The aim of the present study was to examine the strain rate sensitivity of SCC containing recycled fibres and a combination of recycled fibres and polypropylene ones. The steel fibres improve the post-crack response of the matrix under quasi-static conditions, whereas the polypropylene fibres are highly affected in structures subjected to high temperatures. The laboratory experiments were performed with an SHPB apparatus, which is widely applied in investigations of

the strain rate sensitivity of different materials. However, each tested material requires special technique procedures to obtain valid test results. One of the goals of this work was to confirm the correctness of the SHPB technique procedures adopted in previous works [9, 10]. The paper presents an investigation of SCC reinforced with fibres and an analysis of the results compared to previous research data.

2. Test program

2.1. Materials

The SCC specimens containing steel fibres coming from end-of-life tyres and a combination of these fibres and polypropylene ones were experimentally tested. The composition of the fibre-reinforced self-compacting mixes is presented in Table 1. Both types of fibres are shown in Fig. 1. The applied volume ratios for recycled steel fibres and polypropylene fibres were equal to 1.5% and 0.25%, respectively. The characteristic parameters of the considered fibres are collated in Table 2. The quasi-static compressive strength of the plain SCC matrix obtained for four-cylinder specimens (150×300 mm) was 57.7 MPa. An extensive description of the specimen materials, their preparation, and the quasi-static testing procedure can be found in [9, 10].

Table 1. Mix compositions and the quasi-static compressive strengths of the mixes.

Mix	Cement CEM I 42.5R [kg/m^3]	Natural sand (0–2 mm) [kg/m^3]	Coarse aggregate (2–16 mm) [kg/m^3]	Super-plasticiser Glemium Sky 591 [kg/m^3]	Water [kg/m^3]	Steel fibres [%] by volume		w/c	Compressive strength [MPa]
						R	PP		
R-SCC	580	927	695	20.3	223	1.5	–	0.38	53.5 (2)
RPP-SCC						1.5	0.25		52.7 (1)

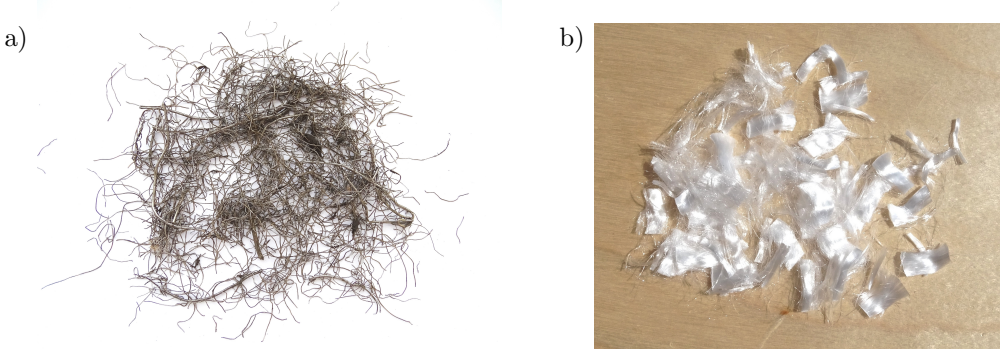

Fig. 1. View of a) recycled steel fibres and b) polypropylene fibres.

Table 2. Properties of the fibres.

Type of fibre	Designation	Length [mm]	Diameter [mm]	Aspect ratio L/D	Tensile strength [MPa]	Modulus of elasticity [GPa]	Density [kg/m^3]
Steel cord (from end-of-life tyres)	R	2–30	0.15 ±5%	∼ 13–200	≥ 2850	210	7.85
Polypropylene	PP	12	0.038	–	440	6.9	0.91

2.2. High strain rate testing

The SHPB technique was used to determine the mechanical properties of fibre-reinforced SCC under high strain rates. The laboratory apparatus adopted in the present investigation consists of 3000 mm long incident and transmitted bars with a diameter of 40 mm, a launcher with a pressure vessel, and a barrel with a 500 mm long striker bar (Fig. 2). All bars were made of steel C45. The pressure generated by the gas launcher accelerated the striker to a velocity range from 10 to 20 m/s during the SHPB tests. The striker impacted the incident bar, through which the elastic wave (ε_i) propagated to the specimen sandwiched between the incident and transmitted bars. At the surface of the specimen, the loading wave was divided into a transmitted (ε_t) and reflected (ε_r) part. The pair of strain gauges placed at the half-length of the incident and transmitted bars measured the waves' profiles.

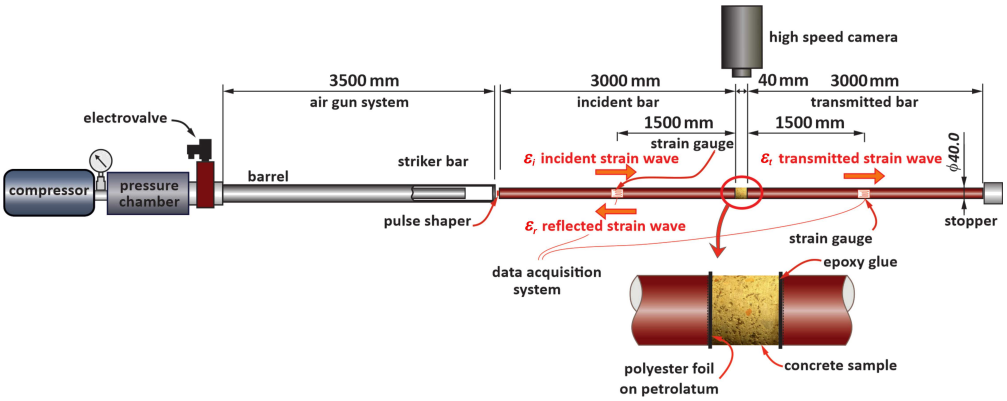

FIG. 2. Scheme of the split Hopkinson pressure bar (SHPB) setup.

The stress (2.1), strain (2.2), and strain rate (2.3) in the specimen were determined according to a one-dimensional wave propagation using the well-known equations:

$$\sigma_1 = \frac{A_A E_A}{A_P}\varepsilon_t(t), \tag{2.1}$$

$$\varepsilon_1(t) = \frac{2c_A}{L}\int_0^t \varepsilon_r(t)\,\mathrm{d}t, \tag{2.2}$$

$$\dot{\varepsilon}(t) = \frac{2c_A}{L}\varepsilon_r(t), \tag{2.3}$$

where L, A_P are the specimen's length and cross-sectional area, respectively, and E_A, A_A, c_A are the pressure bar Young's modulus, cross-sectional area, and elastic wave velocity, respectively.

The deformation and damage process of the specimen under dynamic loading were recorded with a high-speed camera.

In general, the size of the specimen that can be tested in SHPB experiments depends on the diameter of the bars. In the present investigation, twenty cylindrical samples (considering the calibration tests) with lengths and diameters of 40 mm were prepared. The strain rate that can be achieved in the specimen depends on many factors, such as, e.g., specimen dimensions, the mechanical response of the tested material, or the striker impact velocity. In these experiments, the strain rates ranged from $138\ \mathrm{s}^{-1}$ to $198\ \mathrm{s}^{-1}$, for which the equilibrium stress state in the specimen during the tests was achieved, and thus, reliable stress-strain curves were obtained. Concrete is a specific material that requires modifying the shape of the incident wave to achieve an appropriate loading condition. It is important to obtain a suitable rising time of the incident wave, and the pulse shaping technique is therefore usually used [20]. In these studies, an appropriate dimension of the aluminium pulse shaper was experimentally selected for each test to achieve the equilibrium stress state in the specimen. The pulse shaper diameter was 8 mm, and the height was equal to 1.5 mm or 2.5 mm, depending on the striker bar velocity.

In turn, in order to minimise the stress concentrations on the contact surfaces of the sample and bars, the specimen end faces were covered with a thin layer of epoxy resin which hardened over time, filling in the unevenness of the sample. The friction between the contact surfaces of the specimen and the bars was reduced by the petrolatum placed on the bars and a layer of polyethylene foil.

The equilibrium stress state could be verified graphically by showing the axial stresses on the two end faces of the specimen, which were calculated with (2.1) and (2.4), respectively:

$$\sigma_2 = \frac{A_A}{A_P}E_A\left(\varepsilon_i(t) + \varepsilon_r(t)\right). \tag{2.4}$$

The example of the profiles of the incident, reflected, and transmitted stress waves with the equilibrium stress state obtained in the sample is shown in Fig. 3.

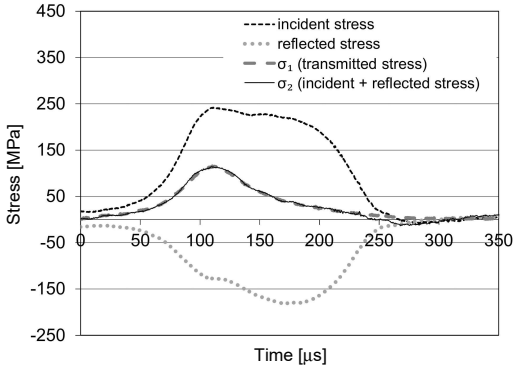

FIG. 3. Equilibrium stress state in the specimen.

The approach to determine the average strain rate of a deforming specimen is presented in Fig. 4. The average value of the strain rate was calculated over the range of the strain rate history curve, which was limited by points obtained from stress-time curves corresponding to 75% of the maximum stress value and the maximum compressive strength of the specimen material, respectively. The above-mentioned method has previously been used in [5, 10].

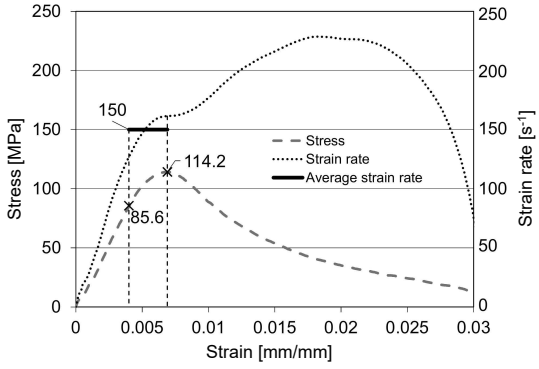

FIG. 4. Determination of the strain rate in the specimen.

3. Split Hopkinson pressure bar (SHPB) tests results

The selected frames from the video recordings presenting the deformation and destruction of the specimens under the SHPB test conditions are collated in Fig. 5.

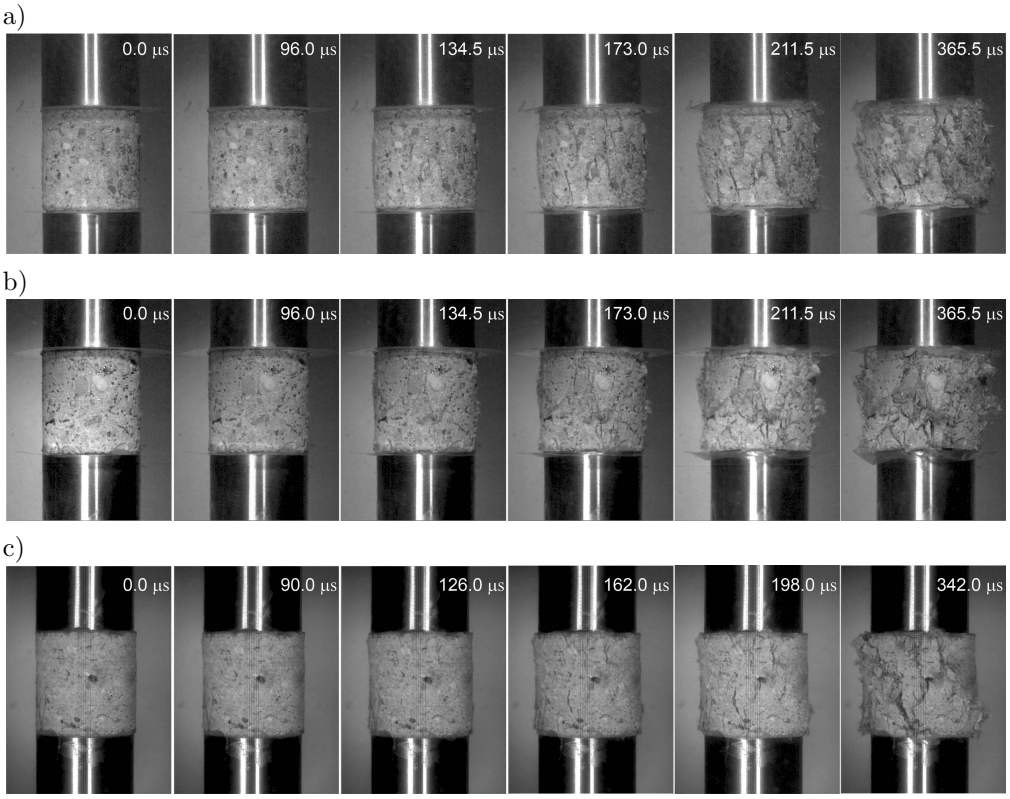

FIG. 5. The deformation and damage process of specimens captured by a high-speed camera: a) R-SCC mixture (165 s^{-1}); b) R-SCC mixture (194 s^{-1}); c) RPP-SCC mixture (144 s^{-1}).

The number of micro- and macro-cracks was higher in specimens containing only recycled fibres (R-SCC mixture Figs. 5a, 5b) than in the RPP-SCC specimen (Fig. 5c). The video records showed that the onset of fragmentation started at about 96 μs and 90 μs for samples R-SCC and RPP-SCC, respectively.

The SHPB technique allowed to obtain the mechanical response of the tested material at high strain rates in the form of the stress-strain curve directly from Eqs. (2.1) and (2.2) after eliminating the time variable. The results obtained for the R-SCC and RPP-SCC mixtures are presented in Figs. 6–8, respectively. The stress-strain curves obtained for each specimen are marked with solid lines, and the average stress-strain curve is marked with a dotted one. Three specimens were investigated under each range of strain rates. The stress-strain relationships obtained in each series were comparable, proving the high accuracy of the tests. The average strain rates achieved in these tests were equal to 165 s^{-1} and 194 s^{-1} for R-SCC (Fig. 6) and 144 s^{-1} for RPP-SCC (Fig. 7). The results are summarised in Table 3, where the coefficient of variation (CV) is also shown in brackets.

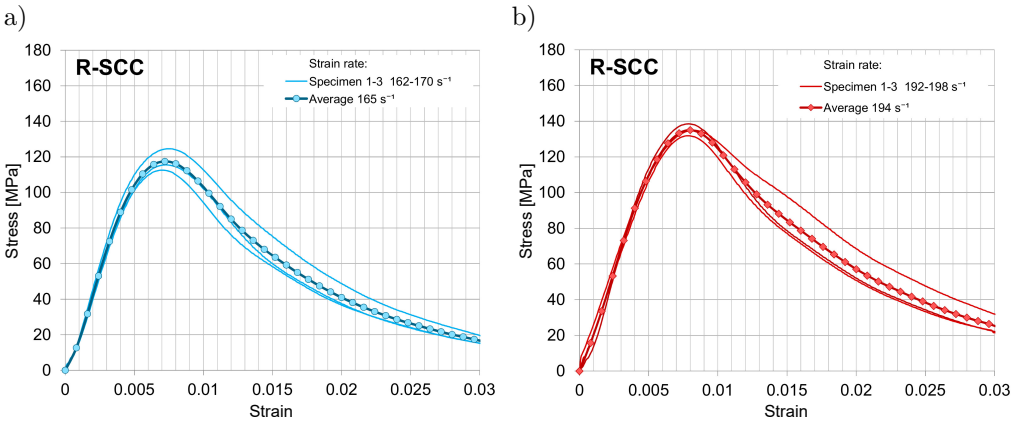

FIG. 6. Dynamic stress-strain curves for the R-SCC mixture tested with average strain rates of: a) 165 s^{-1}; b) 194 s^{-1}.

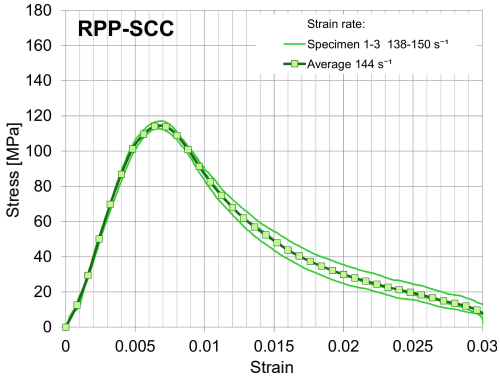

FIG. 7. Dynamic stress-strain curves for the RPP-SCC mixture.

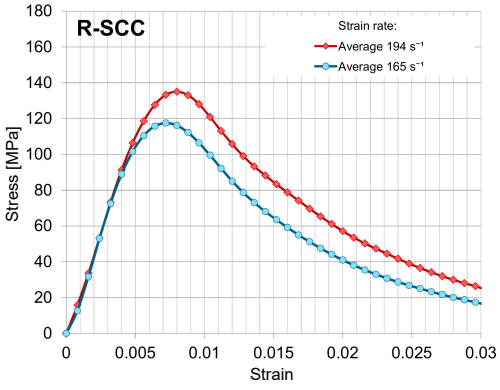

FIG. 8. Comparison of the average dynamic stress-strain curves for the R-SCC mixture.

Table 3. The results of the SHPB compression tests.

Mix	No.	Strain rate [s^{-1}]	Average strain rate [s^{-1}]	Dynamic compressive strength $\varphi_{\chi,\mathrm{dyn}}$ [MPa]	Average dynamic compressive strength [s^{-1}]	Strain at peak stress $\times 10^{-3}$	Average strain at peak stress $\times 10^{-3}$	Quasi-static compressive strength $f_{c,stat}$ [MPa]	DIF	Total absorption energy E [J/m^3]
R-SCC	1	163	165 (3)	124.6	117.6 (5)	0.0076	0.0073 (5)	53.5 (2)	2.33	1.86
	2	162		112.6		0.0069			2.10	
	3	170		115.5		0.0073			2.16	
	1	198	194 (2)	138.5	135.1 (2)	0.0079	0.0080 (3)		2.59	2.31
	2	193		131.9		0.0079			2.46	
	3	192		134.9		0.0083			2.52	
RPP-SCC	1	150	144 (4)	114.2	114.7 (2)	0.0069	0.0068 (2)	52.7 (1)	2.17	1.52
	2	138		117.1		0.0068			2.22	
	3	145		112.9		0.0066			2.14	

A significant increase in compressive strength was observed with the increase of strain rate in the R-SCC mixture. The compressive strength and total absorption energy increased with the strain rate, which could be found by comparing the average stress-strain curves presented in Fig. 8. For the highest strain rate, the dynamic increase factor (DIF; the ratio of dynamic $f_{c,\mathrm{dyn}}$ to quasi-static $f_{c,\mathrm{stat}}$ compressive strength) exceeded 2.5 (Table 3).

The total absorption energy per volume unit was determined from the stress-strain dependency according to Eq. (3.1):

$$E_{\mathrm{absorb}} = \int_0^{\varepsilon_{\mathrm{limit}}} \sigma \, \mathrm{d}\varepsilon, \tag{3.1}$$

where $\varepsilon_{\mathrm{limit}}$ is the strain value corresponding to 5% of the maximum stress on the falling slope of the stress-strain curve (Fig. 9).

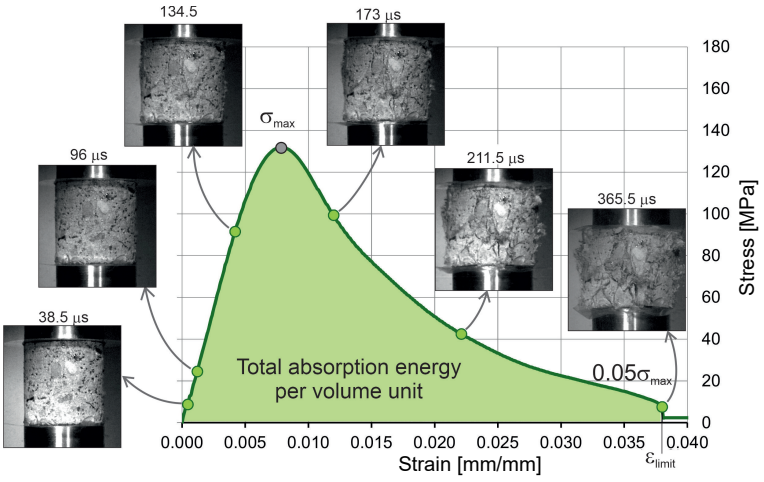

FIG. 9. Determination of the total absorption energy in the specimen.

The above-mentioned value of the upper integration limit was adopted for two reasons. Firstly, the authors wanted to consider the contribution of fibres to the loading energy dissipation process during the post-damage phase. Secondly, when analysing the high-speed camera recordings, it was observed that the specimen fragmentation process was already well advanced at this point, and many free-moving fragments were scattered beyond the space limited by the contact surfaces of the incident and transmitted bars (see Fig. 9) and did not participate in the dissipation of the loading energy.

4. Discussion

4.1. Stress-strain curves

The SCC samples reinforced only with recycled fibres (R-SCC) were subjected to two ranges of strain rates with averages of 165 s^{-1} and 194 s^{-1}. Meanwhile, the specimens in which the recycled steel fibres were mixed with polypropylene ones (RPP-SCC) were deformed with an average strain rate of 144 s^{-1}. Our previous laboratory investigations [10] were performed on R-SCC and RPP-SCC mixtures, which were compressed with an average strain rate of around 100 s^{-1}. The stress-strain curves obtained here and the previous ones [10] are collated in Fig. 10, where for comparison purposes, the mechanical response of the tested material at a quasi-static strain rate ($5.6 \cdot 10^{-5}$ s^{-1}) is also presented and marked with dotted lines.

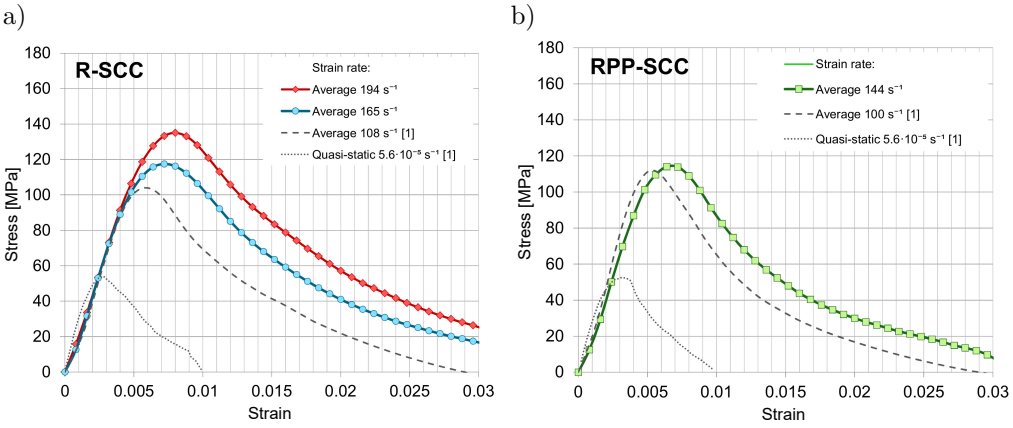

Fig. 10. Comparison of quasi-static and dynamic stress-strain curves for the tested mixtures: a) R-SCC; b) RPP-SCC.

The results of the studies conducted here on the same mixture correspond well with those from previous research for both the R-SCC and RPP-SCC mixtures. An increase in compressive strength with the increase in strain rate was observed for both mixtures (Fig. 10). The negligible influence of the strain rate on the modulus of elasticity in RPP-SCC is shown in Fig. 10b.

To reveal the influence of the polypropylene fibres on the strain rate sensitivity of R-SCC, another stress-strain curves comparison was developed and is presented in Fig. 11. The value of the compressive strengths of the R-SCC and RPP-SCC specimens were comparable for average strain rates of 165 s^{-1} and 144 s^{-1}, especially since the compressive strength of R-SCC would probably have been slightly lower at strain rates of around 140 s^{-1}. Thus, it can be concluded that the strain rate sensitivities of the SCC containing both types of fibres

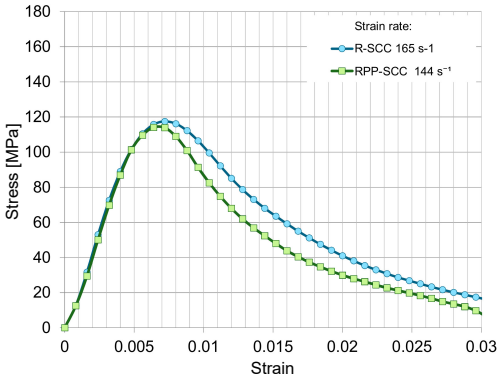

FIG. 11. Comparison of the dynamic stress-strain curves for the RPP-SCC and R-SCC mixtures.

(DIF = 2.18) and the mixture with only one type of fibre (DIF = 2.20) were comparable. It is noteworthy that other researchers have observed a decrease in strain rate sensitivity with a further increase of steel fibre contents [3, 12, 13, 15, 17]. Indeed, although the amount of fibres was increased in this work, polypropylene fibres were introduced which were characterised by different mechanical properties (e.g., Young's modulus) to those of the steel fibres.

The reliability of the SHPB procedures adopted by the authors of this paper for brittle materials was confirmed. It could be concluded on the comparison of the results presented in Sec. 3 of the present paper with the results of the previously performed experiments [10].

Figure 12 compares the strain rate sensitivity of fibre-reinforced concrete obtained here with the results from various works on fibre-reinforced cement-based materials. For comparison, only the DIF values for cement-based materials

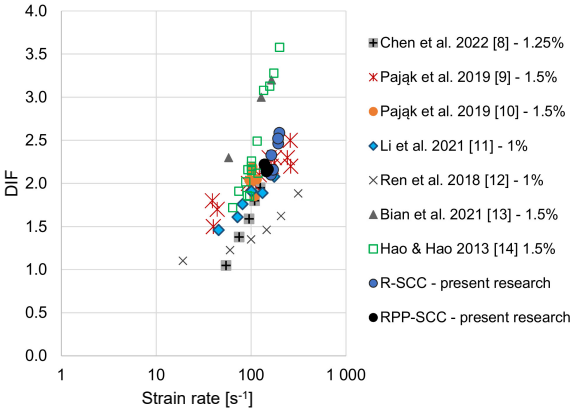

FIG. 12. Comparison of the dynamic stress-strain curves for the RPP-SCC and R-SCC mixtures (the percentage values denote the volume fractions of fibres).

with compressive strengths in a range from 45–145 MPa were chosen [8–14]. Cement-based materials reinforced with steel fibres with a volume fraction in the 1–1.5% range were selected. The DIF values obtained here agree well with the results presented by other researchers [8–14]. The scatter of the results observed in Fig. 12 could be caused by differences in the compressive strength of the matrix [4, 5]. The data scatter may also result from many different factors that are usually related to the preparation of the material specimens (e.g., type of cutting technique, accuracy, and geometric correctness of the specimens), as well as the quality of preparation and execution of SHPB experiments (e.g., bars alignment, parallelism and flatness of the SHPB bars end faces, coaxial striker bar impact, etc.).

4.2. Failure patterns

The degree of destruction of the RPP-SCC and R-SCC specimens subjected to strain rates close to 100 s^{-1} was much lower than in the same specimens deformed at higher strain rates (Fig. 13). Fragmentation was observed as the dominant failure pattern, i.e., the specimens were cracked, but they did not disintegrate, and fragments of them remained between the SHPB bars after the tests. This shows that the fibres in the specimen were able to bridge the cracks, which was also observed in [17]. More fibres were introduced to the RPP-SCC specimens than to the R-SCC mixtures, and therefore the degree of destruction of the RPP-SCC specimens was lower. However, the polypropylene fibres did not affect the value of the compressive strength, only the damage pattern.

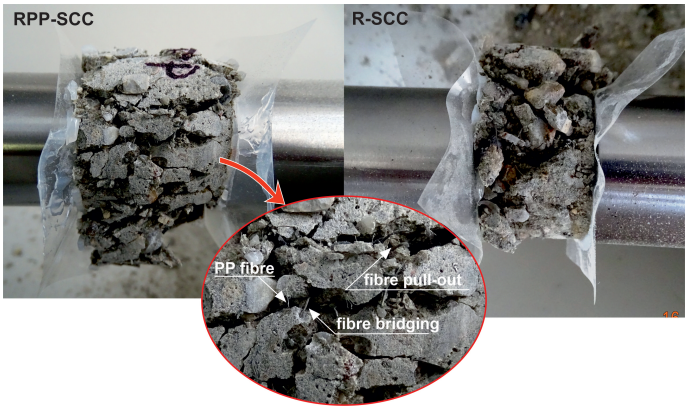

FIG. 13. The failure pattern of the specimens at strain rates of around 100 s^{-1} (images taken from previous tests described in [10]).

The damage to the specimens tested under the highest strain rates was always manifested as pulverisation (Fig. 14). All but some small fragments of the

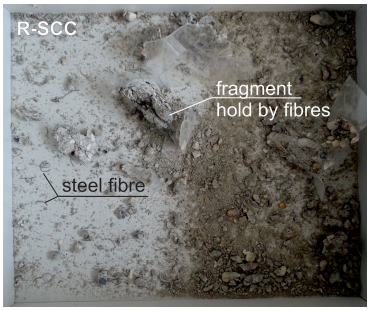

FIG. 14. View of the specimen after the test with a strain rate of 193 s^{-1}.

specimen were completely crushed, indicating that there was not enough time for the fibres to bridge the cracks.

4.3. Limitations of the split Hopkinson pressure bar (SHPB) technique

All materials analysed with the SHPB method require an experimental selection of the suitable testing conditions that would result in obtaining valid test data. In fact, the range of strain rates over which the cement-based materials can be tested using the SHPB technique is quite narrow. An example of this is shown by the results of the preliminary tests presented in Fig. 15. The striker impact velocity chosen in the first shot was too low to generate a loading wave that could damage the specimen. As a result, the strain rate of the specimen only achieved a value of 34 s^{-1}. In turn, the same material specimen subjected to the second shot with a higher striker velocity was damaged, and a strain rate of 112 s^{-1} was observed. The analysis of the results shows that the first shot caused only elastic deformation, which did not affect the structure of the specimen. Therefore, the obtained stress level cannot be treated as the com-

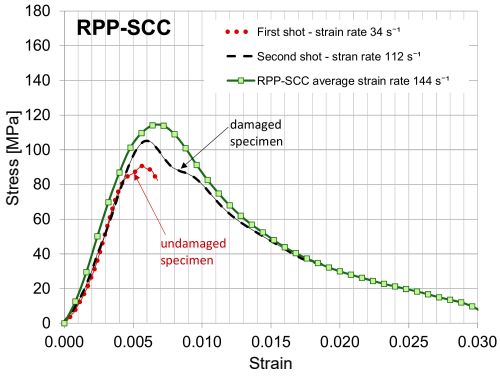

FIG. 15. Comparison of dynamic RPP-SCC stress-strain curves developed according to data from the preliminary and main SHPB tests.

pressive strength of the tested material at a strain rate of 34 s^{-1} because the amplitude of the loading pulse was too small and the loading period too short to damage the specimen before unloading and achieving the maximum strength of the tested material. This proves that determining the compressive strength of the RPP-SCC specimen under strain rates of around 40 s^{-1} would be difficult based on the data obtained from the SHPB experiment.

Testing cement-based materials with the SHPB technique is also problematic when the SHPB tests must be performed at higher strain rates. Cement-based materials are highly strain rate sensitive over a relatively narrow range of strain rates compared to most metals and their alloys. The upper limit of the highest strain rates induced in cement-based specimens is close to 300 s^{-1}. Above this strain rate level, the equilibrium stress state in the specimen is usually very difficult to achieve.

5. Conclusions

This study dealt with the strain rate sensitivity of SCC in which steel fibres from end-of-life tyres and polypropylene fibres were implemented. The experimental data of the high strain rate tests performed with the SHPB technique were presented with previously published test results. The following conclusions can be drawn from their analysis:

- The behaviour of SCC reinforced with recycled fibres (R-SCC) and polypropylene fibres (RPP-SCC) under high strain rates demonstrates its high strain rate sensitivity. A pronounced increase of compressive strength and total energy absorption with an increase of strain rate was observed in both mixtures. For the highest strain rates (around 194 s^{-1}), the DIF value for R-SCC exceeded 2.5. The increase in the total energy absorption of the specimens indicates that both types of mixtures can be used to enhance protective structures.
- The specimens with a combination of recycled and polypropylene fibres (RPP-SCC) exhibited strain rate sensitivities comparable to those of SCC samples reinforced only with recycled steel fibres (R-SCC) in the 144–165 s^{-1} range of strain rates. The DIF values were around 2.2 for both mixtures, and thus, their effectiveness was comparable.
- The addition of polypropylene fibres to the R-SCC mixture influenced the failure patterns of the specimens at lower strain rates (about 100 s^{-1}). The predominant pattern of failure observed in this range was fragmentation, highlighting the role of the fibres in carrying the loads. The application of polypropylene fibres reduced the degree of destruction of the specimens containing only recycled steel fibres. For the highest strain rates, only

pulverisation was observed, potentially indicating a lack of bonds between the fibres and the matrix.

The use of the pulse shaping technique and appropriate specimen preparation, which guarantees geometric correctness, allowed us to obtain valuable results from the SHPB tests while meeting the main methodical requirements, namely reaching the equilibrium stress state in the specimen. However, the SHPB technique has its limitations for testing cement-based materials. In this work, the SHPB technique was applied to investigate SCC specimens reinforced with fibres at strain rates exceeding 40 s^{-1}. The maximum compressive strength of the specimen was not achieved at this strain rate level because the loading wave energy was too low to cause damage to the specimen. On the other hand, according to our own experience, higher strain rates of around 300 s^{-1} can be obtained, and these are limited by the problem of reaching the equilibrium stress state in the specimen.

Acknowledgments

The first author gratefully acknowledges the financial support provided by the scholarship founded by the Rector of the Silesian University of Technology 07/SFW18/003-05/2019 and the Polish Ministry of Education and Science BK-225/RB6/2022. This work was also co-financed by the Military University of Technology in Warsaw under the UGB research project.

References

1. Bragov A.M., Petrov Y.V., Karihaloo B.L., Konstantinov A.Y., Lamzin D. A., Lomunov A.K., Smirnov I.V., Dynamic strengths and toughness of an ultra high performance fibre reinforced concrete, *Engineering Fracture Mechanics*, **110**: 477–488, 2013, doi: 10.1016/j.engfracmech.2012.12.019.

2. Brandt A.M., Fibre reinforced cement-based (FRC) composites after over 40 years of development in building and civil engineering, *Composites Structures*, **86**(1–3): 3–9, 2008, doi: 10.1016/j.compstruct.2008.03.006.

3. Yoo D.-Y., Banthia N., Impact resistance of fiber-reinforced concrete – A review, *Cement and Concrete Composites*, **104**: 103389, 2019, doi: 10.1016/j.cemconcomp.2019.103389.

4. Hao Y., Hao H., Jiang G.P., Zhou Y., Experimental confirmation of some factors influencing dynamic concrete compressive strengths in high-speed impact tests, *Cement and Concrete Research*, **52**: 63–70, 2013, doi: 10.1016/j.cemconres.2013.05.008.

5. Pająk M., Baranowski P., Janiszewski J., Kucewicz M., Mazurkiewicz Ł., Łaźniewska-Piekarczyk B., Experimental testing and 3D meso-scale numerical simulations of SCC subjected to high compression strain rates, *Construction and Building Materials*, **302**: 124379, 2021, doi: 10.1016/j.conbuildmat.2021.124379.

6. Simalti A., Singh A.P., Comparative study on performance of manufactured steel fiber and shredded tire recycled steel fiber reinforced self-consolidating concrete, *Construction and Building Materials*, **266**(Part B): 121102, 2021, doi: 10.1016/j.conbuildmat.2020.121102.

7. Domski J., Katzer J., Zakrzewski M., Ponikiewski T., Comparison of the mechanical characteristics of engineered and waste steel fiber used as reinforcement for concrete, *Journal of Cleaner Production*, **158**: 18–28, 2017, doi: 10.1016/j.jclepro.2017.04.165.

8. Chen M., Si H., Fan X., Xuan Y., Zhang M., Dynamic compressive behaviour of recycled tyre steel fibre reinforced concrete, *Construction and Building Materials*, **316**: 125896, 2022, doi: 10.1016/j.conbuildmat.2021.125896.

9. Pająk M., Janiszewski J., Kruszka L., Laboratory investigation on the influence of high compressive strain rates on the hybrid fibre reinforced self-compacting concrete, *Construction and Building Materials*, **227**: 116687, 2019, doi: 10.1016/j.conbuildmat.2019.116687.

10. Pająk M., Janiszewski J., Kruszka L., Hybrid fiber reinforced self-compacting concrete under static and dynamic loadings, [in:] *Concrete – Innovations in Materials, Design and Structures*, *Proceedings of the fib Symposium 2019*, W. Derkowski *et al.* [Ed.], pp. 766–772, Lausanne, 2019.

11. Li N., Jin Z., Long G., Chen L., Fu Q., Yu Y., Zhang X., Xiong C., Impact resistance of steel fiber-reinforced self-compacting concrete (SCC) at high strain rates, *Journal of Building Engineering*, **38**: 102212, 2021, doi: 10.1016/j.jobe.2021.102212.

12. Ren G.M., Wub H., Fang Q., Liu J.Z., Effects of steel fiber content and type on dynamic compressive mechanical properties of UHPCC, *Construction and Building Materials*, **164**: 29–43, 2018, doi: 10.1016/j.conbuildmat.2017.12.203.

13. Bian L., Ma J., Zhang J., Li P., Dynamic compression behavior and a damage constitutive model of steel fibre reinforced self-compacting concrete, *Advances in Materials Science and Engineering*, **2021**: 8085949, 2021, doi: 10.1155/2021/8085949.

14. Hao Y., Hao H., Dynamic compressive behaviour of spiral steel fibre reinforced concrete in split Hopkinson pressure bar tests, *Construction and Building Materials*, **48**: 521–532, 2013, doi: 10.1016/j.conbuildmat.2013.07.022.

15. Yu Q., Zhuang W., Shi C., Research progress on the dynamic compressive properties of ultra-high performance concrete under high strain rates, *Cement and Concrete Composites*, **124**: 104258, 2021, doi: 10.1016/j.cemconcomp.2021.104258.

16. Jankowiak T., Rusinek A., Voyiadjis G.Z., Modeling and design of SHPB to characterize brittle materials under compression for high strain rates, *Materials*, **13**(9): 2191, 2020, doi: 10.3390/ma13092191.

17. Wang Y., Wang Z., Liang X., An M., Experimental and numerical studies on dynamic compressive behavior of reactive powder concretes, *Acta Mechanica Solida Sinica*, **21**(5): 420–430, 2008, doi: 10.1007/s10338-008-0851-0.

18. Marzec I., Tejchman J., Winnicki A., Computational simulations of concrete behaviour under dynamic conditions using elasto-visco-plastic model with non-local softening, *Computers and Concrete*, **15**(4): 515–545, 2015, doi: 10.12989/cac.2015.15.4.515.

19. Brara A., Klepaczko J.R., Experimental characterization of concrete in dynamic tension, *Mechanics of Materials*, **38**(3): 253–267, 2006, doi: 10.1016/j.mechmat.2005.06.004.

20. Shemirani A. B., Naghdabadi R., Ashrafi M.J., Experimental and numerical study on choosing proper pulse shapers for testing concrete specimens by split Hopkinson pressure bar apparatus, *Construction and Building Materials*, **125**: 326–336, 2016, doi: 10.1016/j.conbuildmat.2016.08.045.

21. Baranowski P., Gieleta R., Malachowski J., Damaziak K., Mazurkiewicz Ł., Split Hopkinson pressure bar impulse experimental measurement with numerical validation, *Metrology and Measurement Systems*, **21**(1): 47–58, 2014, doi: 10.2478/mms-2014-0005.

22. Jankowiak T., Rusinek A., Lodygowski T., Validation of the Klepaczko–Malinowski model for friction correction and recommendations on Split Hopkinson Pressure Bar, *Finite Elements in Analysis and Design*, **47**(10): 1191–1208, 2011, doi: 10.1016/j.finel.2011.05.006.

Received February 18, 2022; accepted version June 24, 2022.